

Advances in Medical Imaging: Aptamer- and Peptide-Targeted MRI and CT Contrast Agents

Anna Koudrina and Maria C. DeRosa*



Cite This: *ACS Omega* 2020, 5, 22691–22701



Read Online

ACCESS |

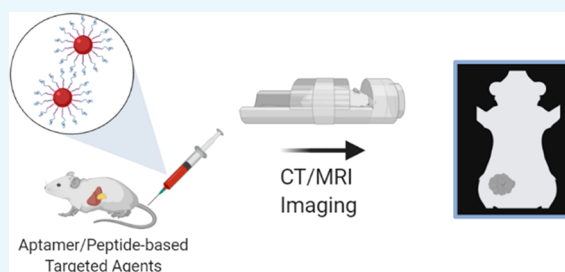


Metrics & More



Article Recommendations

ABSTRACT: Computed tomography (CT) and magnetic resonance imaging (MRI) are among the most well-established modalities in the field of noninvasive medical imaging. Despite being powerful tools, both suffer from a number of limitations and often fall short when it comes to full delineation of pathological tissues. Since its conception, molecular imaging has been commonly utilized to further the understanding of disease progression, as well as monitor treatment efficacy. This has naturally led to the advancement of the field of targeted imaging. Targeted imaging research is currently dominated by ligand-modified contrast media for applications in MRI and CT imaging. Although a plethora of targeting ligands exist, a fine balance between their size and target binding efficiency must be considered. This review will focus on aptamer- and peptide-modified contrast agents, outlining selected formulations developed in recent years while highlighting the advantages offered by these targeting ligands.



1. GENERAL INTRODUCTION

A number of different imaging modalities exist and are currently used to distinguish between physiological and pathological tissues and processes. Since their development, magnetic resonance imaging (MRI) and computed tomography (CT) imaging have revolutionized the field of medical imaging and are among the most well-established technologies in the field.^{1a} Many detailed reviews covering the principles of MRI and CT have been written, including those by Grover et al.^{1b} and Goldman,^{1c} respectively. To allow for better delineation of anatomical structures and differentiation between normal and pathological tissues, contrast materials have been used in both. Gd^{3+} is the most commonly used MRI contrast entity and is administered as part of stable chelates with multidentate ligands, such as diethylenetriaminepentaacetic acid (DTPA), 1,4,7,10-tetraazacyclododecane-1,4,7,10-tetraacetic acid (DOTA), and others.^{1a} Iodinated small molecules consisting of a central 2,4,6-triiodinated benzene ring are among the most commonly used CT contrast agents. In particular, iohexol, sold under the trade name of Omnipaque, and iopimadol, sold as Isovue, are examples of clinical CT contrast agents.^{1a} An in-depth discussion of these, including the currently understood strengths and limitations, can be found in a review written by Wallyn et al.^{1a}

Noteworthy limitations of the conventionally used contrast agents include lack of specificity toward the pathological tissue, rapid clearance which necessitates high administration doses, and toxic effects, especially as it pertains to tissue accumulation.^{1a–c} With that in mind, there has been a major push toward the development of targeted contrast agents in

order to overcome these pitfalls.^{1a} Targeting ligands, such as antibodies, proteins, affibodies, aptamers, peptides, small molecules, and others, have been researched (Figure 1). Generally, antibodies or proteins tend to be the targeting agent of choice. For example, antibodies have been found to be effective in oncological imaging, and a comprehensive review was written by Warram, whereas protein–gadolinium formulations have been utilized for MRI, which was outlined by Vithanarachchi.^{2a,b} Affibodies are another example of an affinity ligand which allows for cancer-associated molecular imaging. They are small (58 amino acids) protein scaffolds engineered to bind a variety of protein targets. In fact, ⁶⁸Ga-labeled affibody molecules have gone as far as phase I/II clinical testing and demonstrated accurate and specific measurement of HER2 expression in positron emission tomography (PET) imaging. A review by Tolmachev and Orlova discusses principles and properties of these molecules.^{2c} Other affibody formulations have been explored, including those useful in MRI, CT, and single-photon emission computed tomography (SPECT).^{2d,e} Nevertheless, peptides and aptamers strike a balance with their properties in comparison to their counterparts. Comparatively, aptamers

Received: June 4, 2020

Accepted: August 18, 2020

Published: September 3, 2020



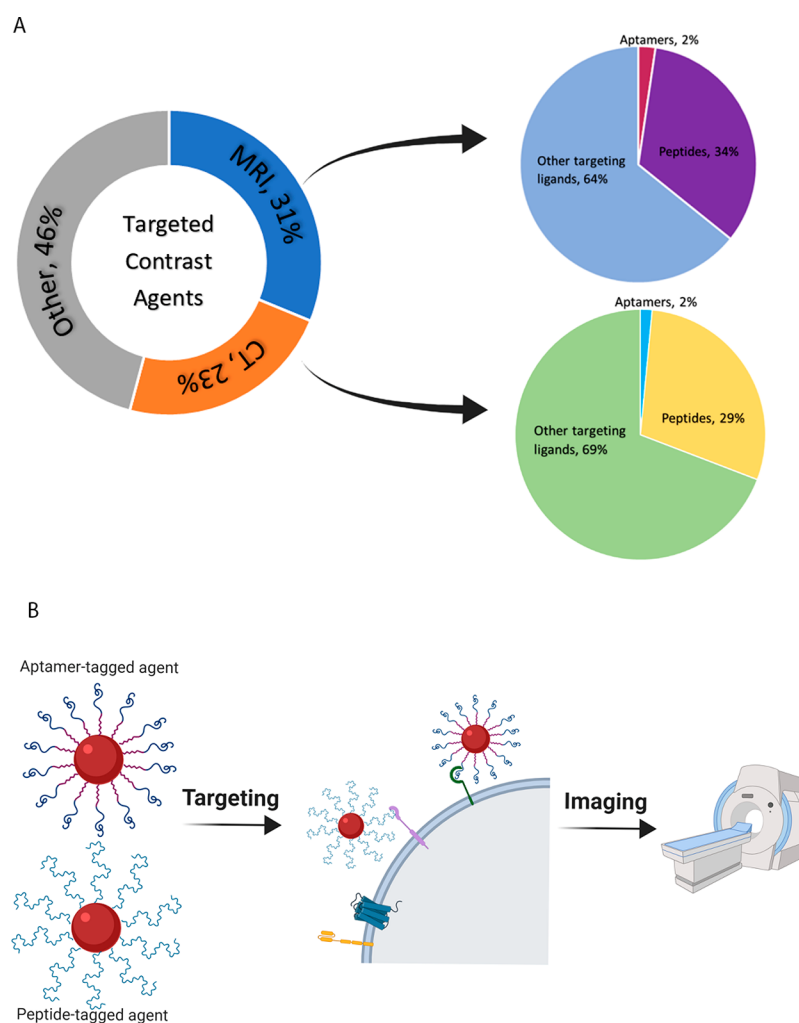


Figure 1. (A) Targeted contrast agents developed toward MRI and CT applications make up more than 50% of the research in the field in the last 3 years. About a third of these utilize peptides or aptamers as their targeting modality. Figure developed based on SciFinder search output. (B) Graphic illustration of aptamer- and peptide-targeted contrast agents for MRI and CT imaging. Image made in BioRender (<https://biorender.com/>).

and peptides demonstrate reasonable clearance times, based on their smaller size, while exhibiting tight target binding to a range of targets, which is not often achieved by small molecules.³ This review will give a basic overview of nano-based approaches for MRI and CT imaging and outline some recent advancements in peptide- and aptamer-targeted imaging agent formulations aimed toward streamlining accurate diagnosis of disease states.

2. NANOCONTRAST AGENTS

In recent years, the development of nanomedicine has taken center stage, demonstrating utility in many areas, including diagnostic imaging. Unsurprisingly, nanoformulations are at the forefront of research toward the development of novel contrast media for medical imaging as they allow for improvement of sensitivity, biocompatibility, and biodistribution.⁴ A major advantage of these formulations is that nanomaterials exhibit the enhanced permeability and retention (EPR) effect. Namely, due to leaky tumor vasculature, nanoformulations can preferentially accumulate in tumor vessels through active or passive targeting while their retention is accomplished based on the lack of functional lymphatic drainage.⁵ In addition, nanoformulations allow for surface

functionalization, which streamlines diagnostic capabilities of various disease states.⁴

One such nanosubstance that has been proposed as an effective MRI contrast agent is superparamagnetic iron oxide nanoparticles (SPIONs). Generally, there are three major factors that dictate efficacy of SPIONs, including particle size, composition, and crystallinity. An important consideration in their design is that SPIONs start to lose their superparamagnetic properties beyond 20 nm in diameter. Overall, iron oxide is extremely susceptible to an external magnetic field based on the presence of 4 or 5 unpaired electrons in the 3D shell for Fe^{2+} or Fe^{3+} states, respectively, with Fe_3O_4 NPs yielding T_2 shortening effect stronger than that of $\gamma\text{-Fe}_2\text{O}_3$.⁶ Unfortunately, with negative contrast agents producing a dark signal, it can at times be difficult to distinguish them from an artifact or an air bubble. Despite these limitations, SPIONs have proven themselves as an effective alternative to other contrast agents as they offer high sensitivity and excellent biocompatibility. Previous commercially available examples include Feridex and Revolist.⁶

Other promising types of MRI nanocontrast agents are gadolinium oxide nanoparticles (Gd_2O_3 NPs), displaying T_1 contrast enhancement superior to that of Gd^{3+} chelates. The

Table 1. Summary of Recently Developed Peptide-Targeted Contrast Agents for Applications in MRI, CT, and Dual Imaging of Various Molecular Markers of Disease

peptide-targeted contrast	imaging target	peptide name	amino acid length	modality	contrast material	injected dose	circulation half-life	ref
exendin-4-dota(ga)-Gd(III) (GdEx)	GLP-1R	Exendin-4	39	MRI	Gd(III)	1.12 μ mol/animal	N/A	12
pHLIP-magnetosomes	tumor extracellular environment	pHLIP	38	MRI	magnetosome (Fe_3O_4)	0.5 mg of Fe/mL or 1.5 mg of Fe/mL	cleared within \sim 24 h	13
NaGdF ₄ @bp-peptide NPs	p32	bp-peptide	9	MRI	NaGdF ₄	10 mg of Gd/kg	N/A	14
FITC-VHP-Fe ₃ O ₄ @SiO ₂	VCAM-1	VHP	7	MRI	Fe ₃ O ₄ @SiO ₂	2.5 mg of NPs/kg	N/A	15
cRGD-GdNPs	$\alpha_v\beta_3$ and $\alpha_v\beta_5$ integrins	cRGD	3	MRI	Gd ₂ O ₃	0.1 mmol Gd/kg	cleared within \sim 24 h	16
T-GNP-ABPs	cathepsin	GB111-NH ₂	3	CT	GNPs	25 mg/mL (5 mg of GNP per mouse)	N/A	17
GNPs-PEG@cNGR	aminopeptidase-N	SH-cNGR	3	CT	GNPs	10 mg/mL	N/A	18
cNGR-Au:Gd@GSH	CD13 receptor	cNGR	3	multimodal (MRI and CT)	Au and Gd atom cluster	5 mM Au, 16 mM Gd	19.33 h	19
pEGFR-targeted Ba ₂ GdF ₇ NPs	EGFR	pEGFR	14	multimodal (MRI and CT)	Ba ₂ GdF ₇	20 mg of Gd/kg	cleared within 24–48 h	20
RGD-PEG-BaGdF ₅	$\alpha_v\beta_3$	RGD	3	multimodal (MRI and CT)	BaGdF ₅	150 mg of Gd/kg	1.26 h	21

function of these nanoparticles is governed by the same principle as the latter, but the enhanced T_1 contrast is based on the high density of Gd^{3+} present within each nanoparticle. A simple example was investigated by Dai and colleagues, assessing the toxicity, pharmacokinetics, biodistribution, and other properties of poly(ethylene glycol) (PEG)-modified Gd_2O_3 NPs.⁷ PEG is a common surface coating used to stabilize nanoparticles, enhance their biocompatibility, and prolong their blood circulation time. This research confirmed that PEGylated Gd_2O_3 NPs display a half-life longer than that of Gd^{3+} chelates, thereby offering greater accumulation at tumor sites, low histological, hepatic, and renal toxicity, and efficient MR contrast enhancement.⁷

Other formulations of MRI nanocontrast agents have been proposed, including ones based on highly paramagnetic ions such as manganese as a possible T_1 agent and dysprosium as a possible T_2 agent. In all cases, as these formulations are nanoparticle-based, the final contrast agent can be surface-modified to produce targeted contrast, dual contrast, or drug-carrying contrast.⁸ Liposomal formulations are an excellent example of substance-carrying nanoparticles, with a surface that can be functionalized, as well as a hollow interior that can be loaded with various molecules. As a result, liposomes can easily act as dual-mode imaging probes and image-guided drug delivery agents. A review written by Xia et al. outlines the design of these probes, geared toward clinical applications.⁹

When considering conventional contrast media in CT, one of the limitations is lack of selectivity between healthy and pathological tissues. Gold nanoparticles (GNPs) are an attractive alternative due to their reactive surface, which allows for incorporation of a large variety of targeting molecules. Other advantages include high X-ray adsorption coefficients, electron density, and atomic number; a combination of these characteristics results in X-ray attenuation, which tends to be stronger than that of iodine-containing molecules.¹⁰ Wang and colleagues designed one such contrast agent consisting of hollow gold nanoparticles (HG NPs) surface-modified with PEG, mPEG@HG NPs. The final mPEG@HG NPs were 63.4 nm in diameter and demonstrated concentration-dependent increase of X-ray attenuation, which was higher than that of the

commercially available control. In vivo imaging further confirmed contrast efficiency while exhibiting good biocompatibility.¹¹ A plethora of other GNP-based contrast agents are being researched, bearing various surface modifications which are often used as another approach to further enhance X-ray attenuation.¹⁰

3. TARGETED CONTRAST FOR MOLECULAR IMAGING

3.1. Peptide Targeting Examples. This section will review the recent examples of MRI, CT, and multimodal formulations which were designed for molecular imaging applications, targeting known pathological markers with peptides that were developed to bind them. Table 1 highlights the important features of these formulations. Not all of these features are discussed in each paper; however, this summary can be used as a guideline for the design of future studies, with these important elements in mind.

A recent example of a novel peptide-targeted MRI probe was published by Clough *et al.*, highlighting the need to quantitatively assess the changes in mass of β -cells, which is associated with the development of diabetes.¹² They proposed employing a peptide, exendin-4, for targeted delivery of the MRI probe. Exendin-4 is composed of 39 amino acids; it is a potent analogue of the peptide which binds to glucagon-like peptide-1 receptor (GLP-1R). As GLP-1R is highly expressed on β -cells, it can be used as a molecular marker. Notably, exendin-4 has shown utility in treatment of diabetes in addition to demonstrating antiapoptotic function. As outlined by the authors, its conjugation to numerous therapeutic and imaging agents has been validated by several groups.¹² In this work, the synthesis and characterization of the exendin-4-conjugated 4-DOTA(ga)-Gd(III) (GdEx) complex as well as its subsequent behavior in vivo using β -cell-depleted C57BL/6J mice were reported. GdEx demonstrated a significantly stronger brightening enhancement when compared to the commercially available $[\text{Gd}(\text{DOTA})]^-$ contrast at the 18–21 min time point and exhibited a slower decline to the baseline value up to the 54 min time point. This was likely correlated with selective accumulation of GdEx in the pancreas from localization to the β -cells. To assess whether GdEx can be used to detect the

decrease in β -cells mass, mouse strain with tamoxifen-inducible, β -cell-specific, Dicer deletion (β Dicer-null) was utilized. β Dicer-null mice exhibited depleted β -cells mass and were strongly hyperglycemic. When injected with GdEx, decreased pancreatic uptake was observed in comparison to the control mice, with the most significant trends evident at 18–21 min (approximately 1.8-fold lower) up to a complete wash-out by 54 min. This proof-of-concept study allows for the development of similar probes that would allow monitoring of physiological changes overtime.¹²

One of the applications of MRI contrast agents is in cancer diagnosis, allowing one to delineate tumor size, shape, and overall location. This information is subsequently used for planning and monitoring of treatment. Schuerle and colleagues proposed targeting of the well-understood extracellular acidity associated with tumors with genetically encoded pH low insertion peptide (pHLIP).¹³ In order to achieve dramatic contrast enhancement, they used magnetosomes, which are particles harvested from magnetotactic bacteria (MTB). Specifically, MTB produce magnetite (Fe_3O_4) in a chain surrounded by a phospholipid bilayer membrane, forming the magnetosome. *Magnetospirillum magneticum* AMB-1 cells were genetically engineered to display pHLIP on the surface of magnetosomes to achieve functionalization. The ability of pHLIP-decorated magnetosomes to bind cells in an acidic environment was tested in vitro using the human breast cancer cell line MDA-MB-231, both at a standard pH of 7.5 and at a slightly acidic pH of 6.5, which is representative of average tumor acidity. Binding of pHLIP-magnetosomes at low pH was shown to be significantly higher than that at neutral pH, as well as when comparing to native magnetosomes at both pH levels. Subsequent in vivo efficiency was tested using mice bearing flank xenografts of the human ductal carcinoma cell line MDA-MB-435S. Intravenous injections were followed by biodistribution assessment at 6 and 24 h postinjection. Approximately 1.5-fold increase of tumoral accumulation was achieved in the presence of pHLIP-functionalized magnetosomes when compared to the control. Finally, a 2.02-fold higher T_2 contrast enhancement was achieved when pHLIP-functionalized magnetosomes preferentially accumulated at the site of the tumor. These results demonstrate that this versatile and flexible platform can be broadly applied toward tumor-selective MRI.¹³

Chen et al. proposed using NaGdF_4 nanoparticle-based formulation to produce a tumor-specific multifunctional nanotheranostic agent.¹⁴ The composite contrast agent consisted of the 9 nm NaGdF_4 core for T_1 -weighted MR imaging, decorated with linearly linked p32 protein binding and pro-apoptotic peptides. More specifically, a tumor-homing motif was designed to target mitochondrial p32, a critical regulator of tumor metabolism, whereas the pro-apoptotic segment produced the therapeutic effect. Cytotoxicity and internalization capabilities of the final complex, denoted NaGdF_4 @bp-peptide NPs, was assessed using human breast cancer cells (MCF-7). Results showed that NaGdF_4 @bp-peptide NPs exerted significant toxic effects on tumor cells, while remaining relatively nontoxic to normal cells. This was related to high targeting efficiency of NaGdF_4 @bp-peptide NPs, which was associated with the presence of the surface recognition elements. Although NaGdF_4 @bp-peptide NPs exhibited relatively low relaxivity values, likely due to the highly branched structure of the peptides, in vitro MRI showed significantly higher signal intensities and cellular internalization in treatments with NaGdF_4 @bp-peptide NPs when compared

to the controls. In vivo studies were conducted using BALB/c mice that were subcutaneously inoculated with MCF-7 cell. Strongly positive MR contrast enhancement was observed at the tumor location in T_1 -weighted images, confirming tumor-targeting capacity of NaGdF_4 @bp-peptide NPs. Finally, ex vivo assessment of the tumor volume confirmed that treatment with NaGdF_4 @bp-peptide NPs results in tumor growth suppression without systemic toxicity. This study reveals that combining targeting and therapeutic elements allows for production of nanotheranostic complexes without compromising the efficacy of either elements.¹⁴

Another example of peptide-targeted contrast agent was formulated to be applied toward atherosclerosis plaque imaging.¹⁵ The vascular cell adhesion molecule 1 (VCAM-1, CD106) is a prominent marker of atherosclerotic plaque development and can therefore be used for targeted diagnosis. In fact, its high expression persists in both early and late stages of atherosclerosis. Peptide-modified magnetic mesoporous silica nanoparticles were developed by Xu et al. Specifically, Fe_3O_4 @ SiO_2 NPs were surface-functionalized with VHPKQHR peptide (FITC-VHP- Fe_3O_4 @ SiO_2), which possesses targeting capabilities toward VCAM-1 that are very analogous to those of an antigen-4. In vitro analysis was conducted using mouse aortic endothelial cells (MAECs) treated with lipopolysaccharide to induce high expression of VCAM-1. The results confirmed that VHP-modified nanoparticles are able to efficiently target atherosclerosis while experiencing low toxicity and good blood compatibility. In vivo imaging was used to confirm targeting and retention of FITC-VHP- Fe_3O_4 @ SiO_2 , following a tail vein injection into ApoE^{-/-} mice that were fed a high-fat diet. This confirmed that FITC-VHP- Fe_3O_4 @ SiO_2 was highly specific toward VCAM-1, whereas a significant reduction in T_2 relaxation time (negative enhancement by approximately 33%) revealed that this type of formulation is superior to commercially available contrast media when used for the diagnosis of atherosclerotic plaques. Finally, targeting capabilities were further reinforced ex vivo using the fluorescence component of FITC-VHP- Fe_3O_4 @ SiO_2 when the aortic vessels were harvested and imaged using 470 nm excitation and 535 nm emission wavelengths. This supports that choosing a molecular marker that is specifically expressed during a particular stage of disease progression could allow for precise monitoring and more effective diagnosis.¹⁵

In a different example of peptide-guided contrast enhancement, ultrasmall gadolinium oxide (Gd_2O_3) nanoparticles (GdNPs) were applied toward targeted tumor imaging. Gadolinium affords these nanoparticles a wide range of properties, including the ability to produce positive MRI contrast (T_1) based on the spin magnetic moment. Ahmad and colleagues proposed coating GdNPs with cyclic RGDs (cRGDs), cyclic arginine-glycine-aspartic acid peptides, for the purposes of targeting tumors through binding to $\alpha_v\beta_3$ and $\alpha_v\beta_5$ integrins overexpressed in tumor angiogenic sites and tumor cells. Both longitudinal and transverse relaxivities of these 1–2.5 nm diameter cRGD-GdNPs were evaluated, demonstrating water-proton relaxivities 3–5 times higher than those of Gd^{3+} -DTPA and Gd^{3+} -DOTA controls. In vitro imaging of U87MG tumor cells confirmed significant internalization of cRGD-GdNPs, which suggests that this type of complex can be used for gadolinium neutron capture therapy. In vivo evaluations were performed using the orthotopic mouse liver tumor model, where nude mice were inoculated with HepG2-luc2 cells. Clear positive contrast enhancement

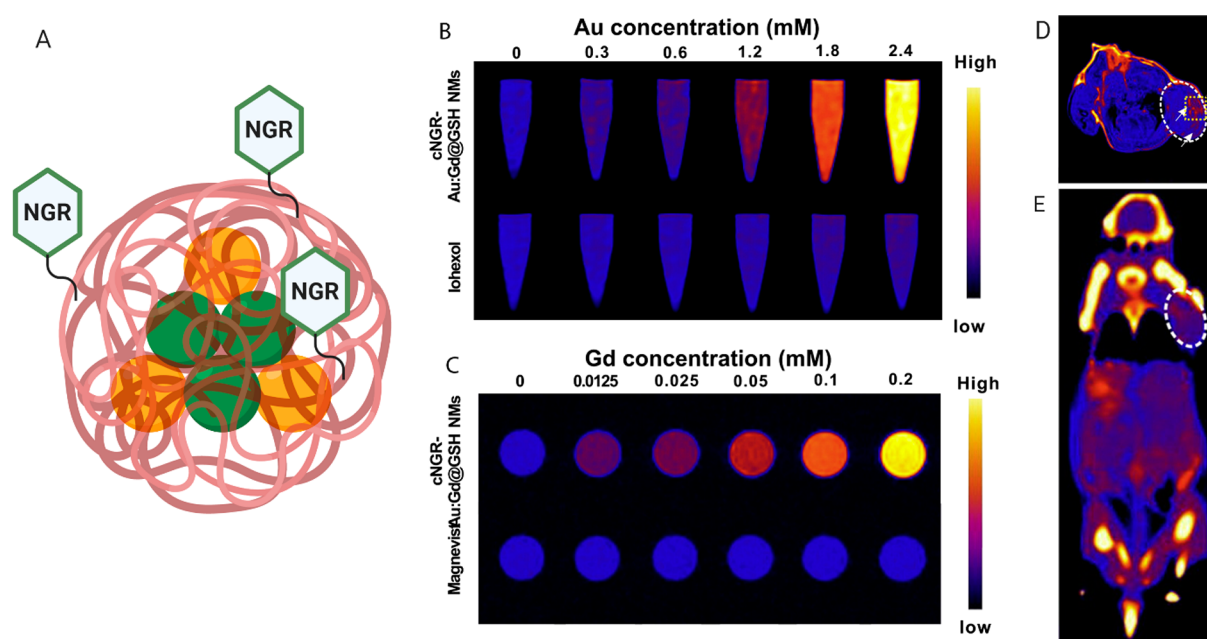


Figure 2. (A) Illustration of the Au:Gd@GSH nanoclusters, labeled with cyclic NGR peptide, used for dual mode imaging, made in BioRender. (<https://biorender.com/>). (B) CT contrast phantom images of cNGR-Au:Gd@GSH NMs compared to iohexol. (C) MR contrast phantom images of cNGR-Au:Gd@GSH NMs compared to Magnevist. (D) MR image of tumor-bearing mouse at 24 h postinjection of Au:Gd@GSH-NGR, with contrast highlighting the location of the tumor in the right shoulder. (E) CT image of tumor-bearing mouse 24 h postinjection of Au:Gd@GSH-NGR, with contrast highlighting the location of the tumor in the right shoulder. Adapted with permission from ref 19. Copyright 2019 Elsevier.

was observed as soon as 5 min postinjection of cRGD-GdNPs, with 3 times higher accumulation at the tumor sites when compared to normal regions of the liver. These results confirmed that Gd-based nanoparticles can be used as MRI contrast agents, and their surface functionalization results in effective targeting.¹⁶

Visualization and characterization of distinct molecular pathways in various disease models allows for assessment of those diseases, which ultimately streamlines early diagnosis and improves prognosis. For example, it has been shown that the activity of cathepsin protease is commonly elevated within tumor microenvironments. Utilizing this unique change within the cancerous tissue, cathepsin targeting can be used for detection and assessment of tumors. This was the goal of Tsvirkun and colleagues, who proposed using surface-modified GNPs as the contrast agent for noninvasive cancer CT imaging.¹⁷ GNPs were modified with a cathepsin inhibitor, GB111-NH₂. GB111-NH₂ is a covalent targeting moiety and is an active site inhibitor specific to cathepsin, thereby acting as an activity-based probe (ABP). The recognition element for cathepsins was the short peptide portion of the probe (carbonyloxy-phenylalanine-lysine), whereas the acyloxymethyl ketone served as a warhead, enabling covalent linkage of the probe to its target. Targeting of GNPs to the tumor site was designed to result in specific accumulation of GNPs, thus increasing contrast and sensitivity of each CT scan. In vitro and in vivo testing was performed using NIH-3T3 and 4T1 cells and BALB/C mice subcutaneously expressing 4T1 cells, respectively. T-GNP-ABPs showed minimal cytotoxicity, as well as size-dependent accumulation in subcutaneous tumors with highest accumulation of up to 12% of the tumor volume for the smaller particles. Interestingly, it was discovered that CT contrast of the tumor was inversely proportional to GNP size and amount of targeting moiety. That is, the 10–30 nm T-GNP-ABPs were the most effective for tumor imaging, based

on their specific tumor uptake. As this study explored different variants of the contrast formulation, testing different sizes of GNPs and variable proportions of the protective PEG coating and GB111-NH₂, it can serve as a guide for future designs of activity-based probes.¹⁷

One of the critical processes in cancer progression is tumor angiogenesis, during which the tumor grows, develops, and eventually metastasizes. Currently, quantitative studies of angiogenesis are based on the measurement of microvascular density, which is calculated using the maximal number of vasculatures per unit area of histological tissue section. This approach is considered to be invasive and unreliable, as it requires an intact tissue sample, and it is not able to account for tissue heterogeneity. Wu and colleagues proposed using CT as a noninvasive method of visualization of tumor vascularization, developing contrast media that allowed for imaging with high sensitivity and specificity and simultaneous high retention.¹⁸ Their formulation was based on surface functionalization of gold nanoparticles with cyclized asparagine-glycine-arginine (SH-cNGR), which was used as the tumor-seeking moiety, and carboxypoly(ethylene glycol)thiol (SH-PEG-COOH) in order to increase circulation time of the contrast media. The final contrast probe, GNPs-PEG@cNGR, was used for targeting aminopeptidase-N (APN/CD13), a peptide overexpressed in the endothelium of tumor angiogenesis. In vitro cytotoxicity and targeting specificity assessments were done using CD13-positive cell lines, HepG2 and HUVEC. Results showed that GNPs-PEG@cNGR had no observable toxic effect on neither tumor nor control tissue which represented microvasculature and renal epithelial cells. In addition, GNPs-PEG@cNGR was able to effectively target CD13, resulting in efficient intracellular accumulation. The effectiveness of the probe as a CT contrast agent was tested in vivo using a subcutaneous xenograft model, targeting 4T1 tumors in mice. The GNPs-PEG@cNGR was able to bind the

Table 2. Summary of the Recently Developed Aptamer-Targeted Contrast Agents for Applications in MR and CT Imaging of Various Molecular Markers of Disease

aptamer-targeted contrast	imaging target	aptamer name	aptamer length (bases)	modality	contrast material	injected dose	circulation half-life	ref
AS1411-G2 (DTPA-Gd)-SS-PR	nucleolin	AS1411	28	MRI	Gd(III)-DTPA	0.1 mmol Gd/kg	N/A	22
G _m LS	tenascin-C	GBI-10	34	MRI	Gd(III)-DTPA-BSA	N/A	N/A	23
M17-SPIONs	matrix metalloproteinase 14	M17	40	MRI	SPIONs	N/A	N/A	24
Den-Apt1	endoglin	endoglin-targeting apt	38	MRI	Gd(III)-DTPA	0.05 mmol Gd/kg	N/A	25
mEND-Fe ₃ O ₄ @CMCS	mouse endoglin	eEND	60	MRI	SPIONs	0.05 mmol Fe/kg	N/A	26
Wy5a-SPIO/Dtxl-NPs	castration-resistant prostate cancer cells	Wy5a	57	MRI	SPIONs	10 mg of Dtxl/kg	controlled drug release for up to 5 days	27
Au-TiO ₂ -A-TTP	nucleolin	AS1411	28	CT	gold	10 mg of Gd/kg	4.71 h	28
Apt-PEG-AuPAMAM-CUR	mucin-1	MUC-1	35	CT	gold	2 mg of CUR/kg	N/A	29
Apt-ALGDG2-iohexol	nucleolin	AS1411	26	CT	iohexol	1.6 μM	N/A	30

tumor vasculature with high specificity, demonstrating rapid and elevated tumor uptake with a 64.9% increase of contrast enhancement of neovascularity after 1 h and 96.5% increase after 4 h.¹⁸

A similar method of assessment of tumor angiogenic activity based on endothelial cell targeting was developed by Li et al.¹⁹ It was proposed that a multimodal contrast agent, utilizing MRI and CT imaging techniques, can be formulated in order to augment tumor vasculature and provide complementary information for a more detailed final assessment. The contrast agent consisted of a gold and gadolinium atom cluster (Au:Gd), coated by a naturally occurring zwitterionic glutathione (GSH) and surface-modified with cyclic NGR peptide (cNGR) (Figure 2A). Au was incorporated to serve as the CT contrast, whereas Gd acted as the MRI contrast, with both ions protected by the outer shell. As in previous formulations, cNGR was used for targeting the CD13 receptor, overexpressed on the tumor surface, to achieve improved cellular binding and tumor retention. Improved longitudinal relaxivity was observed when compared to Magnevist in phantom MRI scans (Figure 2C), and higher X-ray attenuation was evident when compared to iohexol in phantom CT scans (Figure 2B). More specifically, in phantom MRI, T_1 proton relaxation of cNGR-Au:Gd@GSH was approximately 8.6 times higher than that of Magnevist when scanned at the same concentrations, whereas in phantom CT, improvement of X-ray attenuation varied between 18 and 180 times that of iohexol, depending on the CT sequence used. In vitro assessments revealed that cNGR-Au:Gd@GSH experiences highly specific binding toward HepG2 while remaining nontoxic. In vivo MR and CT imaging, using mice with orthotopically implanted EMT-6 cells, clearly demonstrated accumulation of cNGR-Au:Gd@GSH at the tumor sites 8 h postinjection (Figure 2D,E). With both imaging modalities, observable contrast and relative signal intensities were significantly higher than those of the untargeted control treatments. Overall, this formulation displayed high clinical potential, allowing for specific targeting, improved contrast enhancement in both MRI and CT while highlighting tumor angiogenic vessels for at least a 24 h period.¹⁹

Another way to combine the strengths of MRI and CT imaging is through the use of nanoparticles such as Ba₂GdF₇, with the Gd element acting as the MRI contrast and barium (Ba, K-edge = 37.4 keV) element as the CT contrast. Recent research has shown that ultrasmall nanoparticles can be rapidly cleared through the renal system; however, one of the main limitations of ultrasmall nanoparticles is the lack of accumulation at the tumor lesion sites. In order to circumvent this issue, as well as to specifically target the tumor cell surface, Feng and colleagues produced epidermal growth factor receptor (EGFR)-targeted peptide-functionalized Ba₂GdF₇ nanoparticles (pEGFR-targeted Ba₂GdF₇ NPs).²⁰ EGFR was proposed as the target for non-small cell lung cancer cells as it is overexpressed in over 70% of those affected. Ba₂GdF₇ nanoparticles were surface-functionalized with an EGFR-seeking peptide to facilitate targeted delivery of contrast media to the tumor location, resulting in positive tumor targeting MR/CT dual-mode imaging. In vitro testing was conducted using A549 lung carcinoma cells incubated with pEGFR-targeted Ba₂GdF₇ NPs, displaying high affinity. Additionally, pEGFR-targeted Ba₂GdF₇ NPs were compared with a clinical MR contrast agent, displaying longitudinal relaxivity that is nearly double. When comparing pEGFR-targeted Ba₂GdF₇ NPs with clinical CT contrast agent (Omnipaque), it was discovered that, to achieve the same contrast enhancement of 200 HU, pEGFR-targeted Ba₂GdF₇ NPs only needed to be a quarter as concentrated as Omnipaque. Finally, a xenograft A549 lung tumor mouse model was used for assessment of the overall efficacy, as well as pharmacokinetics and toxicity of the pEGFR-targeted Ba₂GdF₇ NPs. It was found that, with increasing time postinjection, the contrast enhancement in both MRI and CT imaging increased, further confirming that pEGFR-targeted Ba₂GdF₇ NPs are specifically accumulated and detained in tumor tissues. Furthermore, the size of pEGFR-targeted Ba₂GdF₇ NPs allowed for efficient elimination from the biological system through the renal pathway, which helps to lower potential toxicity. Overall, this was proven to be a promising nanomaterial in dual-mode imaging, utilizing the advantages of both MRI and CT, as well as functional diversity of peptides,

to be applied toward directed and well-rounded tumor diagnosis and therapy assessment.²⁰

Similar nanoparticles containing gadolinium and barium ions, BaGdF₅ NPs, were investigated by Wang et al. for targeted dual-mode imaging of angiogenic tumor vasculature.²¹ The surface of the nanoparticles was modified with a $\alpha_v\beta_3$ -targeting tripeptide, RGD. This allowed for targeting of $\alpha_v\beta_3$, the integrin adhesion molecule that is universally overexpressed in the endothelial cells of angiogenic tumor vasculature. Even at high concentrations, RGD-PEG-BaGdF₅ NPs demonstrated negligible cytotoxicity when tested against HUVEC cells in vitro. In vivo testing of RGD-PEG-BaGdF₅ NPs did not result in any apparent histopathological abnormalities or lesions in the heart, liver, spleen, lungs, or kidneys, further confirming good biocompatibility. When testing the ability of RGD-PEG-BaGdF₅ NPs to produce sufficient contrast enhancement, HU and 1/T₁ values were compared to those of iohexol and Gd-DTPA, respectively. The slope of the linear increase of HU in relation to RGD-PEG-BaGdF₅ NPs' concentration was calculated to be 5.626 HU mM⁻¹, which is higher than that of iohexol at 3.799 HU mM⁻¹. Similarly, the r₁ value of RGD-PEG-BaGdF₅ NPs was calculated to be 1.584 mM⁻¹s⁻¹ and compared to 4.255 mM⁻¹s⁻¹ of Gd-DTPA, demonstrating MR T₁ contrast performance, albeit weaker than that of Gd-DTPA. Dual-modal contrast performance and tumor vasculature targeting was assessed in vivo, showing highest contrast enhancement at 0.5 h time point for both CT and MR imaging. Furthermore, RGD-PEG-BaGdF₅ NPs demonstrated highest enrichment in the reticuloendothelial system-rich organs, specifically accumulating in the tumor sites within 3 h.²¹

3.2. Aptamer-Targeted Contrast. Aptamers are selected through a process of systematic evolution of ligands by exponential enrichment (SELEX) and are single-stranded oligonucleotides with propensity to bind their targets with high affinity and selectivity. They offer several advantages over other commonly used targeting ligands that can be utilized in the formulation of contrast agent for MRI and CT imaging. These advantages are based on their small size, non-immunogenic nature, tight and specific target binding, and ease of synthesis and handling.^{22–26} As above, Table 2 highlights some of the important aspects that were highlighted in the research described in this section. These can be used as recommendations for important elements of testing in the future development of aptamer-targeted contrast agents.

Zu and colleagues recently developed a macromolecular MRI contrast agent using polyrotaxanes, which are cyclic molecules threaded onto a polymer “axle” and capped with bulky end caps.²² One of the advantages of polyrotaxanes is their prolonged blood circulation, as they are not as readily internalized by macrophages as small molecules. The proposed structure consisted of disulfide bonds located at the terminal ends of the molecule. These bonds are readily cleaved in the cytoplasm, thus resulting in dethreading of the overall structure into smaller subunits and subsequent elimination. The system was modified with an aptamer (AS1411) that is specific to a highly overexpressed multifunctional surface–protein, nucleolin. Testing demonstrated that longitudinal relaxivity of the novel complex was double that of the clinically used Gd³⁺-DTPA contrast agent. Additionally, AS1411-G2(DTPA-Gd)-SS-PR demonstrated superior biocompatibility, not eliciting accumulation-associated toxicity when it was tested against HUVAC. Targeting ability of AS1411, designed to enhance

MRI performance, was confirmed in vitro and in vivo using MCF-7 cells overexpressing nucleolin on the surface and a subcutaneous tumor-bearing mouse model, respectively. Faster accumulation at the tumor site and longer contrast imaging time confirmed that this formulation may be a good candidate for clinical applications for tumor imaging.²²

In another example, a DNA aptamer (GBI-10) that specifically binds tenascin-C (TN-C), an extracellular glycoprotein highly expressed on the surface of solid tumor tissues in the brain, breast, uterus, ovaries, prostate, pancreas, colon, stomach, mouth, larynx, and many others, was utilized. In order to improve the binding of GBI-10, as well as enhance contrast-associated relaxivity in MRI, Zhang et al. prepared gadolinium-loaded liposomes that were surface-modified with iso-nucleoside-modified GBI-10 (GBI-10_m), G_mLs.²³ In order to further improve relaxivity of this novel contrast formulation, paramagnetic lipid Gd-DTPA-BSA was incorporated into the membrane of the liposomes. As expected, in T₁-weighted MR images, G_mLs produced a signal intensity higher than that of the controls or Gd-DTPA at similar concentrations. Targeting abilities were assessed in vitro using MDA-MB-435s cells, which are human breast duct cells overexpressing TN-C, and fluorescently modified G_mLs for simple visualization. Fluorescence intensity of the cells incubated with G_mLs was 2 times higher than that of control incubations. Additionally, cellular uptake of G_mLs was observed, confirming that TN-C(+) cells were susceptible to G_mLs internalization. It was evident that the presence of the aptamer in the final liposomal formulation, G_mLs, resulted in higher targeting, thereby improving specificity. In addition, the liposomal preparation itself allowed for increased contrast production based on the presence of higher Gd concentrations. Additionally, choosing an appropriate aptamer not only resulted in targeting of the surface-expressed receptors but also facilitated liposomal uptake into the tumor.²³

Matrix metalloproteinase 14 (MMP14) is a cellular marker that can be used to detect pancreatic cancer, hepatocellular carcinoma, lung carcinomas, gastrointestinal carcinomas, breast carcinomas, gliomas, and cervical carcinomas. The Huan group was able to select a DNA aptamer, M17, using MMP14-transfected 293T cells.²⁴ In vivo fluorescence imaging, utilizing MIA PaCa-2 tumor-bearing BALB/c mice, was used to confirm that M17 is able to specifically recognize MMP14-positive cells. They subsequently utilized M17 in surface functionalization of magnetic nanoparticles (Fe₃O₄) for MRI imaging. T₂ values of the control cell as well as control aptamer incubations were compared to those of M17-SPIONs and MMP14-transfected 293T incubation, with values significantly higher for the latter. Overall, targeted delivery resulted in high specificity and high affinity of SPIONs toward MMP14 marker, confirming that this formulation is a promising targeting agent with potential to be used for targeted diagnosis and treatment of MMP14-positive cancers.²⁴

It is commonly accepted that early cancer detection is crucial for optimized therapeutic response. Whereas hepatocellular carcinoma (HCC) is readily diagnosed in its late stage with the help of MRI and CT imaging, detection of lesions smaller than 2 cm, associated with early stages of this cancer, is 47% or less. Yan and colleagues proposed an aptamer-functionalized formulation in order to improve the detection of these tiny HCC lesions, thereby improving the prognosis of HCC patients.²⁵ The final contrast nanoprobe used endoglin targeting in order to image small-volume HCCs with high

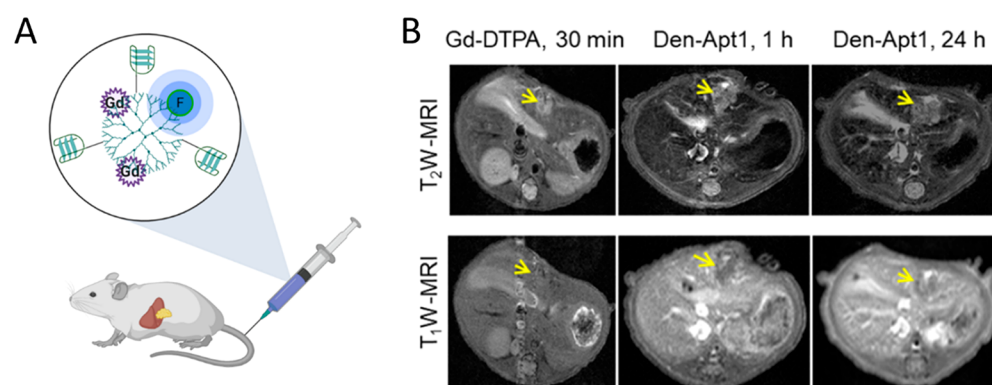


Figure 3. (A) Illustration of the dendrimer system, labeled with Gd chelate, a NIR fluorophore, and the endoglin-targeting aptamer, made in BioRender. (<https://biorender.com/>). (B) Sample T_1 - and T_2 -weighted MR imaging of hepatocellular carcinoma xenografts at 1 h (middle) and 24 h post-treatment with Den-Apt1 (right) compared to conventional agent Gd-DTPA (left). Adapted with permission from ref 25. Copyright 2018 American Chemical Society.

sensitivity and specificity. Endoglin is a marker that is overexpressed on the vascular endothelium of solid tumors. The selected endoglin-specific aptamer was conjugated to Gd^{3+} -DTPA, as well as near-infrared fluorophore IR783 on a G5 dendrimer scaffold, denoted Den-Apt1 (Figure 3A). MRI phantom imaging was used to confirm the capability of Den-Apt1 to produce contrast, demonstrating linear correlation between its increasing concentration and relaxation rates in T_1 -weighted imaging. The fluorescent component of the probe was used to confirm targeting efficiency of Den-Apt1 toward HCC cell lines in vitro, displaying significantly higher intracellular signal 2 h post-treatment when compared the untargeted control. In vivo studies were conducted using nude mice bearing orthotopic hepatic tumor xenografts and Den-Apt1 as well as Den-PEG injected through an i.v. When the contrast signal of Den-Apt1 was compared with that of Gd^{3+} -DTPA, the T_1 signal associated with Den-Apt1 was substantially higher at the tumor margins after 30 min (Figure 3B). After 1 and 24 h postinjections, the tumor area became more enhanced, owing its contrast to the endoglin-mediated tumor uptake of Den-Apt1. Finally, ex vivo optical imaging was used to further verify the biodistribution of Den-Apt1, confirming its accumulation at the site of HCC (Figure 3B). Overall, this nanoprobe allows for effective delineation of the tumor surface, holding promise toward guided tiny HCC surgery.²⁵

Zhong et al. proposed a different variation of endoglin-targeting MRI contrast agent. Their group selected an aptamer that specifically bound to mouse endoglin (mEND) on murine neovascular endothelial cells. The final nanoprobe consisted of the superparamagnetic Fe_3O_4 producing T_2 contrast and carboxymethyl chitosan (CMCS) as the wrapping agent to ensure biocompatibility and reduced toxicity (as mEND- Fe_3O_4 @CMCS).²⁶ As previously, the mEND aptamer was to serve as the recognition molecule, ensuring that the Fe_3O_4 @CMCS contrast would be specifically delivered toward the target. The final 87 nm nanoprobe was tested to confirm targeting ability, as well as contrast enhancement. In vitro experiments confirmed that mEND- Fe_3O_4 @CMCS nanoparticles could specifically bind to vascular endothelial cells expressing endoglin with superior targeting ability as compared to controls. When MR signals were compared, mEND- Fe_3O_4 @CMCS produced significantly enhanced signal in T_2 -weighted imaging at the same concentration as unmodified Fe_3O_4 . In

vivo experiments, using HCC-bearing mice injected with mEND- Fe_3O_4 @CMCS, confirmed that this nanoprobe is able to produce enhanced contrast at the tumor site. This confirms that targeting of MR contrast agent can improve specific imaging of HCC tumors.²⁶

Fang et al. recently reported an aptamer-conjugated formulation using multifunctional polymeric nanoparticles for applications in advanced prostate cancer-targeted MRI and controlled drug delivery. An aptamer, Wy5a, was selected through cell-SELEX to specifically bind castration-resistant prostate cancer cells (PC-3). Self-assembly method, using a prefunctionalized triblock copolymer (PLGA-*b*-PEG-*b*-Wy5a), was utilized to produce “core-shell” nanoparticles that encapsulated superparamagnetic iron oxide nanoparticles (SPION) and docetaxel (Dtxl). SPION was used to produce negative contrast in T_2 -weighted scans, whereas Dtxl, a chemotherapeutic drug for CRPC, was used for controlled treatment. Initial assessment of contrast enhancement capabilities showed that encapsulation of SPION did not reduce the associated magnetization effects. In fact, their clustering resulted in significant T_2 relaxation shortening with relaxivity values approximately 2-fold higher than that of the commercially available Resovist. In vitro testing confirmed that Wy5a-SPION/Dtxl-NPs are able to produce significantly enhanced negative contrast associated with selective internalization achieved through Wy5a targeting PC-3 cells. Wy5a-SPION/Dtxl-NPs also demonstrated controlled drug release with significantly higher cytotoxicity when compared to nontargeted counterpart or Dtxl alone; IC_{50} was 1.42-fold and 1.27-fold lower than those of the nontargeted counterpart and Dtxl, respectively. In vivo antitumor efficacy was also confirmed through significant tumor regression achieved in the presence of Wy5a-SPION/Dtxl-NPs. It is evident that multifunctional formulations like this one are a promising class of targeted drug and contrast delivery systems.²⁷

A handful of recent examples are centered around the use of aptamers as targeting moieties in CT imaging. These formulations are developed based on the previously underlined principle of high atomic number elements, such as gold and iodine, experiencing high X-ray attenuation. One such complex was devised by Cao et al., using a combination of gold nanocrystals grown on TiO_2 nanosheets and targeting elements, including mitochondria-targeted triphenylphosphine (TPP) and AS1411 aptamer.²⁸ These components were used

to achieve multifunctionality in therapeutic and imaging applications. Specifically, incorporating noble metals such as gold has been shown to improve the quantum yield of reactive oxygen species in sonodynamic therapy. Conveniently, gold can then be used to trace the TiO₂-based nanoagents and assess their utility as sonosensitizers. In this case, the aforementioned AS1411 aptamer was used for targeting of the cancer cell membrane through nucleolin, whereas TPP was used to assist in delivery to and accumulation in the mitochondria. In the context of sonodynamic therapy, Au-TiO₂-A-TPP was tested both *in vitro* and *in vivo*, resulting in complete tumor growth suppression. For CT monitoring, increasing concentrations of Au-TiO₂-A-TPP exhibited a linear relationship with X-ray attenuation values (CT value, HU) and increasingly observable brightening contrast. Bright contrast was observed at the location of the tumor when 10 mg/kg of Au-TiO₂-A-TPP was administered through an *i.v.* to MCF-7 tumor-bearing female BALB/c nude mice, confirming the ability of Au-TiO₂-A-TPP to selectively accumulate due to targeting. This type of multifunctional formulation can be reproduced with different targeting elements for applicability toward other types of cancer cells.²⁸

In a different study, Alibolandia and colleagues investigated the use of poly(amidoamine) (PAMAM) G5 dendrimers for encapsulation of curcumin and GNPs (a formulation the foundation of which is similar to that reported by Yan et al.²⁵) as a targeted multifunctional theranostic nanoplatform.²⁹ Tumor tissue targeting was achieved through the use of MUC-1 aptamer, which selectively binds to mucin-1 receptors overexpressed during angiogenesis and tumorigenesis in a number of cancers, including colorectal, breast, lymphocytic leukemia, adrenal cell, and prostate carcinomas. Curcumin is a naturally occurring polyphenol which provides anti-inflammatory and anti-neoplastic effects; however, its poor aqueous solubility, low bioavailability, and high blood clearance require its delivery in an appropriate vehicle. This study evaluated the ability of Apt-PEG-AuPAMAM-CUR to selectively target mucin-1, thereby delivering curcumin while synchronously providing CT contrast. Both *in vitro*, using MUC-1 positive cell lines (HT29 and C26), and *in vivo*, using subcutaneously developed colorectal adenocarcinoma (C26 cell line) in BALB/C mice, studies were utilized to investigate targeting efficiency and cellular toxicity of Apt-PEG-AuPAMAM-CUR. When compared to controls, treatments with Apt-PEG-AuPAMAM-CUR resulted in selective targeting, which elicited significantly higher cytotoxicity. Attenuation capabilities of Apt-PEG-AuPAMAM-CUR were assessed *in vivo* after *i.v.* administration. Highly localized contrast enhancement was observed and attributed to aptamer-targeted delivery of Apt-PEG-AuPAMAM-CUR to the tumor site. Through utilization of different targeting elements, this technology would allow for accurate diagnosis, specific delivery of therapeutic agents, and monitoring of therapeutic response of different adenocarcinomas.²⁹

Mohammadzadeh and co-workers explored a different type of aptamer-decorated dendrimer as a nanocarrier for CT contrast material.³⁰ Specifically, anionic linear globular dendrimer G2 (ALGDG2) was loaded with conventionally used CT contrast agent, iohexol, and surface-functionalized with the AS1411 aptamer. As above, AS1411 was used for targeting cancer cells, and the main objectives were to decrease off-target toxicity and reduce dosage required for significant contrast enhancement. Off-target effects such as cytotoxicity

and apoptosis were tested *in vitro* using nucleolin-positive human breast cancer cells, MCF-7 and HEK-293, as the control cell line. The overall observed trend showed that non-encapsulated iohexol and untargeted ALGDG2-iohexol, but not Apt-ALGDG2-iohexol, elicited cytotoxicity on HEK-293 cells after 72 h. Further, Apt-ALGDG2-iohexol produced a toxic effect on MCF-7 cells. This was supported when apoptosis was observed after treatment of HEK-293 cells with iohexol and ALGDG2-iohexol. Targeting efficiency was also confirmed, demonstrating significantly higher uptake of Apt-ALGDG2-iohexol when compared to its untargeted counterparts. *In vivo* studies using 4T1-tumor-bearing female BALB/c mice were conducted to assess imaging ability and to further confirm targeting efficiency. After *i.v.* administration of Apt-ALGDG2-iohexol into the tail vein, tumor sites were clearly visible in spiral CT imaging after 20 min. Histopathological assessments were performed by harvesting kidney, spleen, liver, and tumor tissues, as well as blood, and no considerable toxicity was observed. This type of design opens doors for other applications in the field of cancer molecular imaging.³⁰

4. CONCLUSIONS

It is evident that incorporation of a targeting ligand into currently existing contrast materials allows for overall higher contrast enhancement and targeted visualization of different components of disease states. Throughout the research outlined above, both peptides and aptamers demonstrated excellent targeting abilities, allowing for optimized biodistribution, while remaining nonimmunogenic. Their superior selectivity results in contrast accumulation at the target of interest, thereby eliciting improved enhancement when compared to commercially available contrast media. As each of the targeting ligands are selected specifically, off-target effects were shown to be limited.

It is expected that, in the future, there will be more ligands selected toward other targets and incorporated into formulations consisting of contrast elements. These formulations will likely not only be targeted but also have the ability to be used as a dual-mode contrast or theranostics, facilitating confirmation of diagnosis through several different imaging modalities or allowing for integration of precise diagnostics and therapeutics, respectively. A number of controls are described within these studies and could be used as guidelines for future research. *In vitro* testing helps determine cytotoxicity and preliminary binding efficiency of the formulations. Here, it is important to test cell lines that display the target of interest and are indicative of the tissue of interest. In addition, off-target toxicity should be assessed through the use of cell lines that represent the suspected route of clearance. *In vivo* assessment should be conducted after distal injections using animals that can express human cell lines, whereas controls for these treatments can include contrast formulations that are either untargeted or modified with a scrambled sequence.

■ AUTHOR INFORMATION

Corresponding Author

Maria C. DeRosa – Department of Chemistry, Carleton University, Ottawa, ON K1S 5B6, Canada; orcid.org/0000-0003-1868-6357; Email: maria.derosa@carleton.ca

Author

Anna Koudrina – Department of Chemistry, Carleton University, Ottawa, ON K1S 5B6, Canada

Complete contact information is available at:
<https://pubs.acs.org/10.1021/acsomega.0c02650>

Notes

The authors declare no competing financial interest.

Biographies

Anna Koudrina received her Bachelor of Science, Honours, in Biochemistry/Biotechnology from Carleton University in 2016. She is currently a chemistry Ph.D. student, with specialization in Chemical and Environmental Toxicology. She is working on developing and characterizing aptamer conjugates to be used in MRI and CT imaging. If successful, these conjugates can be used to improve the current methods of diagnosis of thrombosis. She is a recipient of a Natural Sciences and Engineering Council of Canada (NSERC) Postgraduate Fellowship.



Prof. Maria C. DeRosa is a professor in the Department of Chemistry at Carleton University. She earned her Ph.D. in 2003 with Prof. Robert Crutchley at Carleton University and was an NSERC Postdoctoral Fellow at the California Institute of Technology in the laboratory of Prof. Jacqueline Barton from 2004 to 2005. Since returning to Carleton in 2005, she heads the Canada Foundation for Innovation (CFI)-funded Laboratory for Aptamer Discovery and Development of Emerging Research (LADDER) where she is focused on the use of aptamer technology for applications in diagnostics and therapeutics. She has been a recipient of the John Charles Polanyi Prize and the Ontario Early Researcher Award.

ACKNOWLEDGMENTS

A.K. and M.C.D. acknowledge the Natural Sciences and Engineering Council of Canada (NSERC) for a Postgraduate Scholarship and Discovery Grant Funding, respectively.

REFERENCES

(1) For selected reviews which discuss the principles of selected imaging modalities and their respective contrast agents, see: (a) Wallyn, J.; Anton, N.; Akram, S.; Vandamme, T. F. *Biomedical Imaging: Principles, Technologies, Clinical Aspects, Contrast Agents, Limitations and Future Trends in Nanomedicines. Pharm. Res.* **2019**, *36* (6), 1–34. (b) Grover, V. P. B.; Tognarelli, J. M.; Crossey, M. M. E.; Cox, I. J.; Taylor-robinson, S. D.; Mcphail, M. J. W. *Magnetic Resonance Imaging: Principles and Techniques: Lessons for Clinicians. J. Clin. Exp. Hepatol.* **2015**, *5* (3), 246–255. (c) Goldman, L. W. *Principles of CT and CT Technology. J. Nucl. Med. Technol.* **2007**, *35* (3), 115–128. (d) Ramalho, J.; Semelka, R. C.; Ramalho, M.; Nunes, R. H.; AlObaidy, M.; Castillo, M. Gadolinium-Based Contrast Agent Accumulation and Toxicity: An Update. *Am. J. Neuroradiol.* **2016**, *37* (7), 1192–1198. (e) Andreucci, M.; Faga, T.; Serra, R.; De Sarro, G.; Michael, A. Update on the Renal Toxicity of Iodinated Contrast Drugs Used in Clinical Medicine. *Drug, Healthcare Patient Saf.* **2017**, *9*, 25–37.

(2) For selected reviews which discuss other targeting ligands used in imaging, see: (a) Warram, J.; de Boer, E.; Sorace, A.; Chung, T.; Kim, H.; Pleijhuis, R.; van Dam, G.; Rosenthal, E. Antibody Based Imaging Strategies of Cancer. *Cancer Metastasis Rev.* **2014**, *33* (0), 809–822. (b) Vithanarachchi, S. M.; Allen, M. J. Strategies for Target-Specific Contrast Agents for Magnetic Resonance Imaging. *Curr. Mol. Imaging* **2012**, *1* (1), 12–25. (c) Tolmachev, V.; Orlova, A. Affibody Molecules as Targeting Vectors for PET Imaging. *Cancers* **2020**, *12* (3), 651. (d) Gao, J.; Chen, K.; Miao, Z.; Ren, G.; Chen, X.; Gambhir, S. S.; Cheng, Z. Affibody-Based Nanoprobes for HER2-Expressing Cell and Tumor Imaging. *Biomaterials* **2011**, *32* (8), 2141–2148. (e) Ståhl, S.; Gräslund, T.; Eriksson Karlström, A.; Frejd, F. Y.; Nygren, P. Å.; Löfblom, J. Affibody Molecules in Biotechnological and Medical Applications. *Trends Biotechnol.* **2017**, *35* (8), 691–712.

(3) Chen, Z.; Wang, Y.; Lin, Y.; Zhang, J.; Yang, F.; Zhou, Q.; Liao, Y. Advance of Molecular Imaging Technology and Targeted Imaging Agent in Imaging and Therapy. *BioMed Res. Int.* **2014**, *2014*, 1–12.

(4) Rosen, J. E.; Yoffe, S.; Meerasa, A.; Verma, M.; Gu, F. X. Nanotechnology and Diagnostic Imaging: New Advances in Contrast Agent Technology. *J. Nanomed. Nanotechnol.* **2011**, *2* (5), 1–12.

(5) Nakamura, Y.; Mochida, A.; Choyke, P. L.; Kobayashi, H. Nanodrug Delivery: Is the Enhanced Permeability and Retention Effect Sufficient for Curing Cancer? *Bioconjugate Chem.* **2016**, *27* (10), 2225–2238.

(6) Li, L.; Jiang, W.; Luo, K.; Song, H.; Lan, F.; Wu, Y.; Gu, Z. Superparamagnetic Iron Oxide Nanoparticles as MRI Contrast Agents for Non-Invasive Stem Cell Labeling and Tracking. *Theranostics* **2013**, *3* (8), 595–615.

(7) Dai, Y.; Wu, C.; Wang, S.; Li, Q.; Zhang, M.; Li, J.; Xu, K. Comparative Study on in Vivo Behavior of PEGylated Gadolinium Oxide Nanoparticles and Magnevist as MRI Contrast Agent. *Nanomedicine* **2018**, *14*, 547–555.

(8) Pellico, J.; Ellis, C. M.; Davis, J. J. Nanoparticle-Based Paramagnetic Contrast Agents for Magnetic Resonance Imaging. *Contrast Media Mol. Imaging* **2019**, *2019*, 1–13.

(9) Xia, Y.; Xu, C.; Zhang, X.; Ning, P.; Wang, Z.; Tian, J.; Chen, X. Liposome-Based Probes for Molecular Imaging: From Basic Research to the Bedside. *Nanoscale* **2019**, *11*, 5822–5838.

(10) Mahan, M. M.; Doiron, A. L. Gold Nanoparticles as X-Ray, CT, and Multimodal Imaging Contrast Agents: Formulation, Targeting, and Methodology. *J. Nanomater.* **2018**, *2018*, 1–15.

(11) Wang, R.; Deng, J.; He, D.; Yang, E.; Yang, W.; Shi, D.; Jiang, Y.; Qiu, Z.; Webster, T. J.; Shen, Y.; et al. PEGylated Hollow Gold Nanoparticles for Combined X-Ray Radiation and Photothermal

Therapy in Vitro and Enhanced CT Imaging in Vivo. *Nanomedicine* **2019**, *16*, 195–205.

(12) Clough, T. J.; Baxan, N.; Coakley, E. J.; Rivas, C.; Zhao, L.; Leclerc, I.; Martinez-Sanchez, A.; Rutter, G. A.; Long, N. J. Synthesis and in Vivo Behaviour of an Exendin-4-Based MRI Probe Capable of β -Cell-Dependent Contrast Enhancement in the Pancreas. *RSC Dalton Trans.* **2020**, *49* (15), 4732–4740.

(13) Schuerle, S.; Furubayashi, M.; Soleimany, A. P.; Gwisai, T.; Huang, W.; Voigt, C.; Bhatia, S. N. Genetic Encoding of Targeted Magnetic Resonance Imaging Contrast Agents for Tumor Imaging. *ACS Synth. Biol.* **2020**, *9*, 392–401.

(14) Chen, Y.; Fu, Y.; Li, X.; Chen, H.; Wang, Z.; Zhang, H. Peptide-Functionalized NaGdF₄ Nanoparticles for Tumor-Targeted Magnetic Resonance Imaging and Effective Therapy. *RSC Adv.* **2019**, *9* (30), 17093–17100.

(15) Xu, W.; Zhang, S.; Zhou, Q.; Chen, W. VHPKQHR Peptide Modified Magnetic Mesoporous Nanoparticles for MRI Detection of Atherosclerosis Lesions. *Artif. Cells, Nanomed., Biotechnol.* **2019**, *47* (1), 2440–2448.

(16) Ahmad, M. Y.; Ahmad, M. W.; Cha, H.; Oh, I.-T.; Tegafaw, T.; Miao, X.; Ho, S. L.; Marasini, S.; Ghazanfari, A.; Yue, H.; et al. Cyclic RGD-Coated Ultrasmall Gd₂O₃ Nanoparticles as Tumor-Targeting Positive Magnetic Resonance Imaging Contrast Agents. *Eur. J. Inorg. Chem.* **2018**, *2018*, 3070–3079.

(17) Tsvirkun, D.; Ben-Nun, Y.; Merquiol, E.; Zlotver, I.; Meir, K.; Weiss-Sadan, T.; Matok, I.; Popovtzer, R.; Blum, G. CT Imaging of Enzymatic Activity in Cancer Using Covalent Probes Reveal a Size-Dependent Pattern. *J. Am. Chem. Soc.* **2018**, *140*, 12010–12020.

(18) Wu, M.; Zhang, Y.; Zhang, Y.; Wu, M.; Wu, M.; Wu, H.; Cao, L.; Li, L.; Li, X.; Zhang, X. Tumor Angiogenesis Targeting and Imaging Using Gold Nanoparticle Probe with Directly Conjugated Cyclic NGR. *RSC Adv.* **2018**, *8*, 1706–1716.

(19) Li, X.; Wu, M.; Wang, J.; Dou, Y.; Gong, X.; Liu, Y.; Guo, Q.; Zhang, X.; Chang, J.; Niu, Y. Ultrasmall Bimodal Nanomolecules Enhanced Tumor Angiogenesis Contrast with Endothelial Cell Targeting and Molecular Pharmacokinetics. *Nanomedicine* **2019**, *15* (1), 252–263.

(20) Feng, Y.; Chen, H.; Shao, B.; Zhao, S.; Wang, Z.; You, H. Renal-Clearable Peptide-Functionalized Ba₂GdF₇ Nanoparticles for Positive Tumor-Targeting Dual-Mode Bioimaging. *ACS Appl. Mater. Interfaces* **2018**, *10*, 25511–25518.

(21) Wang, T.; Jia, G.; Cheng, C.; Wang, Q.; Li, X.; Liu, Y.; He, C.; Chen, L.; Sun, G.; Zuo, C. Active Targeted Dual-Modal CT /MR Imaging of VX₂ Tumors Using PEGylated BaGdF₅ Nanoparticles Conjugated with RGD. *New J. Chem.* **2018**, *42*, 11565–11572.

(22) Zu, G.; Cao, Y.; Dong, J.; Zhou, Q.; van Rijn, P.; Liu, M.; Pei, R. Development of an Aptamer-Conjugated Polyrotaxane-Based Biodegradable Magnetic Resonance Contrast Agent for Tumor-Targeted Imaging. *ACS Appl. Bio Mater.* **2019**, *2*, 406–416.

(23) Zhang, L.-X.; Li, K.-F.; Wang, H.; Gu, M.-J.; Liu, L.-S.; Zheng, Z.-Z.; Han, N.-Y.; Yang, Z.-J.; Fan, T.-Y. Preparation and In Vitro Evaluation of a MRI Contrast Agent Based on Aptamer-Modified Gadolinium-Loaded Liposomes for Tumor Targeting. *AAPS PharmSciTech* **2017**, *18* (5), 1564–1571.

(24) Huang, X.; Zhong, J.; Ren, J.; Wen, D.; Zhao, W.; Huan, Y. A DNA Aptamer Recognizing MMP14 for in Vivo and in Vitro Imaging Identified by Cell-SELEX. *Oncol. Lett.* **2019**, *18*, 265–274.

(25) Yan, H.; Gao, X.; Zhang, Y.; Chang, W.; Li, J.; Li, X.; Du, Q.; Li, C. Imaging Tiny Hepatic Tumor Xenografts via Endoglin-Targeted Paramagnetic/Optical Nanoprobe. *ACS Appl. Mater. Interfaces* **2018**, *10*, 17047–17057.

(26) Zhong, L.; Zou, H.; Huang, Y.; Gong, W.; He, J.; Tan, J.; Lai, Z.; Li, Y.; Zhou, C.; Zhang, G.; Li, G.; Yang, N.; Zhao, Y. Magnetic Endoglin Aptamer Nanoprobe for Targeted Diagnosis of Solid Tumor. *J. Biomed. Nanotechnol.* **2019**, *15* (2), 352–362.

(27) Fang, Y.; Lin, S.; Yang, F.; Situ, J.; Lin, S.; Luo, Y. Aptamer-Conjugated Multifunctional Polymeric Nanoparticles as Cancer-Targeted, MRI-Ultrasensitive Drug Delivery Systems for Treatment

of Castration-Resistant Prostate Cancer. *BioMed Res. Int.* **2020**, *2020*, 1–12.

(28) Cao, Y.; Wu, T.; Dai, W.; Dong, H.; Zhang, X. TiO₂ Nanosheets with the Au Nanocrystal-Decorated Edge for Mitochondria-Targeting Enhanced Sonodynamic Therapy. *Chem. Mater.* **2019**, *31*, 9105–9114.

(29) Alibolandi, M.; Hoseini, F.; Mohammadi, M.; Ramezani, P.; Einafshar, E.; Taghdisi, S. M.; Ramezani, M.; Abnous, K. Curcumin-Entrapped MUC-1 Aptamer Targeted Dendrimer-Gold Hybrid Nanostructure as a Theranostic System for Colon Adenocarcinoma. *Int. J. Pharm.* **2018**, *549* (1–2), 67–75.

(30) Mohammadzadeh, P.; Cohan, R. A.; Ghoreishi, S. M.; Bitarafan-Rajabi, A.; Ardestani, M. S. AS1411 Aptamer-Anionic Linear Globular Dendrimer G2-Iohexol Selective Nano-Theranostics. *Sci. Rep.* **2017**, *7* (1), 1–16.